ILASS 2008
Sep. 8-10, 2008, Como Lake, Italy

Paper ID ILASS08-1-10

EFFERVESCENT ATOMIZER: INFLUENCE OF THE OPERATION CONDITIONS AND INTERNAL GEOMETRY ON SPRAY STRUCTURE; STUDY USING PIV-PLIF

Jan Jedelsky*, Michael Landsmann*, Miroslav Jicha*, Ivo Kuritka°

*Brno University of Technology, Technicka 2896/2, 61669 Brno, Czech Republic
°Tomas Bata University in Zlin, Nam. T. G. Masaryka 5555, 760 01 Zlin, Czech Republic
Tel.: +420 541 143 266, Fax.: +420 541 143 365, e-mail: jedelsky@fme.vutbr.cz

ABSTRACT
A single-hole effervescent atomizer spraying light heating oil (LHO) with air as atomizing medium in "outside-in" gas injection configuration was studied using PIV-PLIF. Influence of operation conditions and atomizer internal design on 2D droplet velocity field, liquid phase concentration and liquid flux in the spray was investigated. Inlet pressure and gas-to-liquid-ratio (GLR) were varied. Several design parameters were modified: size and number of aeration holes, their location, diameter of mixing chamber and discharge orifice shape.
Increase of GLR in examined range 2-10 % leads to increase of the droplet velocity in entire radial profile but particularly near the spray axis and to decrease of spray cone half-angle for all atomizer configurations. Increase in atomization pressure in the range 0.1 - 0.5 MPa causes increase of velocity through all radial profile and indistinctive expansion or reduction of the half-angle depending on atomizer design.
The spray cone half-angle ranges 8.8° to 14.6° for all measured configurations and operation conditions. The half-angle increases with: reduction of exit orifice length/diameter ratio, enlargement of aeration area, decrease of aeration hole size and decrease in mixing chamber length. Influence of aeration chamber diameter is not consistent. Influence of atomizer geometry on droplet velocity distribution is reasonable.

INTRODUCTION

Droplet size is usually the most observed and important parameter when designing atomizer. Spray structure can be an additional requirement for some applications; the distribution of liquid mass within a spray is of importance in reacting sprays where local heat release rate and species concentration depends on the radial distribution of fuel. The spray structure is given by a distribution of liquid mass and by drop velocity field. Several papers deal with effect of the atomizer operation conditions on liquid distribution [1, 2] and on spray cone angle [3-6]. Works [4, 5] describe influence of some atomizer geometrical parameters on the spray cone angle. Velocity field and its variation with atomizer operation conditions are frequently alluded but no information is available in the literature on the effect of atomizer internal geometry [7].

Various techniques are employed for study of the spray structure. Visual spray observation supported by a photographic documentation has been often used for determination of the spray cone angle [3] and for qualitative description of the liquid breakup [8, 9]. Focused-image holography [9, 10] or x-ray radiography and tomography [11] enable to get into the optically dense structure of spray in the near nozzle region. Mechanical patternation is frequent and simple method to measure liquid distribution within the spray [1]. Optical measurement methods as Planar Laser-Induced Fluorescence (PLIF) are useful in fast determination of the liquid concentration distribution within the spray [12]. Particle Image Velocimetry (PIV) serves for planar droplet velocity measurement. Simultaneous PIV and PLIF measurements enable to determine a liquid mass flux distribution.

Chen and Lefebvre [3] examined the spray cone angles produced by a plain-orifice effervescent atomizer using several fluids with different viscosities and surface tensions. Measurements of the visible spray cone angle were carried out over wide ranges of both air injection and ambient air pressures and GLR. Obtained results show that the effervescent sprays have substantially wider cone angles than those produced by plain-orifice pressure atomizers. In general, spray angles are widened by reductions in liquid viscosity and surface tension and by increases in atomizing air injection pressure. GLR shows more complex influence. Whitlow and Lefebvre [1] measured radial liquid distribution in the effervescent spray of water/air mixture and found effective cone angles of about 23° for operation in the bubbly flow regime with GLR 1.2 % and 16° in annular flow regime with GLR 12 %. Wade et al. [4] studied spray cone angle using atomizers with exit orifice diameter in the range 0.18 to 0.3 mm in the range of GLR 0.015 to 0.32 and injection pressure 12 to 33 MPa. They found that spray cone angle increases with increase in GLR and injection pressure. Minor influence of the orifice size was reported. Sovani et al. [5] described the structure and steady-state performance of an effervescent Diesel injector. They studied, among others, the influence of exit orifice diameter, aerator pore size, atomizing gas-liquid ratio, and injection pressure on spray cone half-angle. Their data show that spray cone half-angle ranges from 7 to 11°, regardless of aerator pore size, exit orifice diameter, GLR or injection pressure. Sovani et al. [6] studied cone angles of effervescent spray in high ambient density environments for different injection pressures, atomizing GLR, and ambient pressures. They found that cone half-angle lies between 5.8 and 11.5° over the entire range of independent parameters studied, and increases linearly with increasing injection pressure or GLR at all ambient pressures. The cone angle first decreases when the ambient pressure increases from 0.27 to 1.5 MPa, but then increases as ambient pressure rises from 1.5 to 5.5 MPa. Jedelsky and Jicha [2] measured radial distribution of the time-averaged and fluctuating liquid

fluctuating liquid concentration and mass flux in the spray of light heating oil. They found both the time-averaged concentration and mass flux profiles narrows with increase in GLR in the measured range 2 - 50 %. Liquid concentration (mass flux) profile increases with the operation pressure in the range 0.2 - 0.5 MPa but anomalous tendency with a maximum at 0.1 MPa was seen and explained by an unsteady spray at this regime. Temporal fluctuations of the liquid concentration and mass flux, related to spray unsteadiness, vary significantly with operation pressure and GLR.

Spray mean drop velocity and drop velocity distribution is important in reacting spray as it influences mixing of the fuel with surrounding air and transport of the reactants into the flame zone. Effect of injection pressure and GLR on the velocity profiles in effervescent spray was studied e.g. by Panchagnula and Sojka [13] and Jedelsky et al. [14]. The papers show that drop velocity increases with increasing injection pressure and with increase in GLR. A maximum of the drop velocity is placed in the spray centerline and the maximum fall out with increase in both radial distance from the centerline and in axial distance from the the atomizer exit orifice. Similar results on the influence of operation conditions are adverted also by other researchers.

Above listed publications provide important information on the spray structure of effervescent atomizers however deeper knowledge of the effect of atomizer internal design on liquid distribution and velocity field is desirable. Our study was undertaken to address this objective.

EXPERIMENTAL APPARATUS

The experimental equipment includes an effervescent atomizer, a cold test bench with fluid supply system and PIV-PLIF system.

Atomizer description. Single-hole, plain orifice atomizer is fed with LHO and uses air as the atomizing medium in the "outside-in" gas injection configuration (Fig. 1). It consists of a cylindrical body in which an aerator tube is inserted. The aerator is connected with an exit nozzle. The liquid (oil) enters the central part of the aerator from left side, while the air is injected into the liquid, through a set of small holes in the aerator envelope. Both fluids form a two-phase mixture, flow downstream and exit the atomizer through a discharge orifice to the ambient atmosphere in the form of a spray. A volume of mixing chamber formed inside the aerator tube is given by the length downstream of the last row of air holes (l_c) and the internal diameter of the aerator tube (d_c). The length l_c, diameter d_c together with the span length. Δl, diameter d_a and number of aeration holes, n are varied in this study. Several atomizers were manufactured for testing; their dimensions can be seen in Table 1. The exit orifice diameter, d_o, was fixed to 2.5 mm, length of the exit orifice, l_o, was varied. There was a conical junction with the apical angle 2β = 120° in front of the orifice.

Table 1. Atomizers tested

Atom.	l_o (mm)	l_c (mm)	Δl (mm)	d_c (mm)	d_a (mm)	n (-)	X^a (-)
	Relative mixing distance $r_{lc} = l_c/d_c$						r_{lc}
E41	0.7	33	20	14	1.0	12	2.4
E42	0.7	53	20	14	1.0	12	3.8
E43	0.7	83	20	14	1.0	12	5.9
E44	0.7	103	20	14	1.0	12	7.4
	Relative mixing chamber diameter $r_{dc} = d_c/d_o$						r_{dc}
E45	0.7	85	30	6	1.0	30	2.4
E46	0.7	85	30	8	1.0	30	3.2
E47	0.7	73	50	14	1.0	24	5.6
	Relative aeration area $r_a = n(d_a/d_o)^2$						r_a
E48	0.7	90	30	5.5	0.6	60	0.017
E49	0.7	85	25	5.5	1.3	18	0.056
E50	0.7	90	25	5.5	1.5	13	0.077
	Relative area of single aeration hole $r_n = 1/n$						r_n
E51	0.7	33	90	14	1.0	40	6.40
E52	0.7	53	50	14	1.0	24	3.84
E53	0.7	63	20	14	1.0	12	1.92
E54	0.7	73	10	14	1.0	8	1.28
	Relative length of the exit orifice $r_o = l_o/d_o$						r_o
E55	0.4	33	90	14	1.0	40	0.16
E56[b]	4.0	33	90	14	1.0	40	1.60
E57	3.0	33	90	14	1.0	40	1.20
E58	0.2	33	90	14	1.0	40	0.08

[a] X means nondimensional parameter varied during tests.
[b] atomizer E56 has exit orifice in the shape of Laval nozzle.

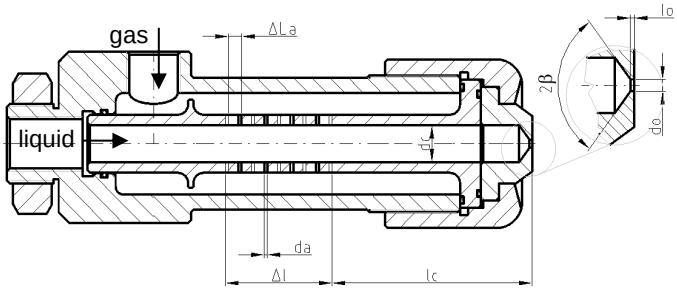

Fig. 1: Schematic layout of the research atomizer.

Atomizers were continuously operated and studied in the vertical downward position of the main axis. The LHO has dynamic viscosity 0.0185 kg/m s, density 874 kg/m^3 and surface tension 0.0297 kg/s^2 at room temperature. The air and oil supplies are controlled separately. Since one of the goals of this study was to investigate how the spray structure depends on the atomizer operation conditions, experiments were performed for several air gauge pressures and GLR values. Both fluids temperatures, gauge pressure and volumetric flow rates were measured, GLR was calculated. Temperatures of both the fluids were kept at 20 ± 2 °C. Description of the test bench and the fluid supply system along with other details on the atomizer operation can be found in [15].

PIV-PLIF system. Double pulsed Nd:YAG Continuum SLII-10 laser equipped with 4th harmonic generator provides two pulses of UV radiation at 265 nm with duration of app. 4 ns. The laser light is converted to a vertical light sheet of app. 100 mm width and 1 mm thickness, which defines the measurement plane. The light sheet illuminates the spray in a plane of the spray axis. The image capture system consists of TSI PIVCAM 13-8 camera and 28 mm lens with appropriate optical filters. Camera axis is perpendicular to the light sheet. The camera and laser are controlled by PC using synchronizer.

Data evaluation: The camera records a set of double LIF images, each from one of the laser pulses. The images are processed with a PIV algorithm to provide a 2-component vector velocity field. The LIF intensity images represent a

liquid concentration $c(x,y)$ in the cross section (x,y) parallel to the spray axis. Images are compensated for attenuation of light sheet in the spray, as described later. Mean concentration image is acquired by averaging of a series of 256 images recorded for each experiment. The images are processed using TSI Insight and MATLAB7 software. Data of the axial velocity component, $w(x,y)$, combined with the concentration image leads to planar liquid mass flux in axial direction:

$$\dot{m}(x,y) = w(x,y)\cdot c(x,y) \qquad (1)$$

Radial profiles of the axial and radial velocity, liquid mass concentration and axial liquid mass flux in the axial distance 100 mm from exit orifice are obtained from corresponding images and used for subsequent evaluation. Normalized cumulative radial distribution of the mean liquid mass concentration is calculated as:

$$c_{ci} = \frac{\sum_{j=1}^{j=i} c_j r_j \Delta r_j}{\sum_{j=1}^{j=n} c_j r_j \Delta r_j} \qquad (2)$$

where r_j is radial distance of the pixel j from spray centerline with the concentration c_j and Δr_j is a thickness of the annulus which corresponds to the width of pixel j. The normalized liquid mass concentration distribution, c_c, is used for determination of the spray borders. A value 75 % of the total normalized cumulative mean liquid mass concentration defines a spray concentration half-angle:

$$\alpha/2 = tg^{-1}(x/y) \qquad (3)$$

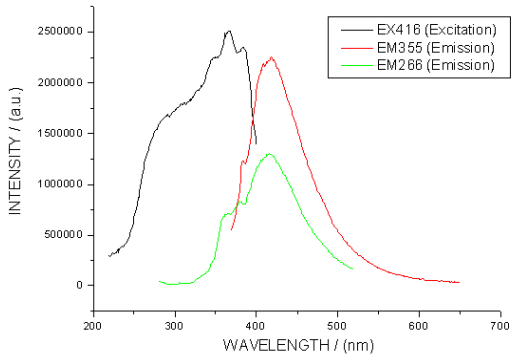

Fig. 2: Emission spectra for excitation wavelength 266 nm and 355 nm and fluorescence yield at 416 nm as a function of the excitation wavelength.

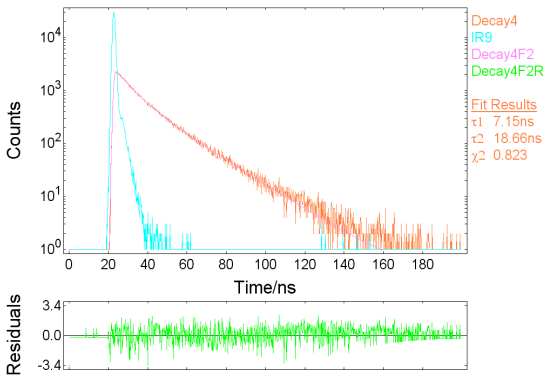

Fig. 3: Lifetime of the fluorescence for excitation pulse 7 ns at 266 nm (top). Residuals of model distribution (bottom).

where x is radial distance covering 75 % of the liquid mass measured at axial distance y = 100 mm. Normalized cumulative mean liquid mass flux, m_c, is calculated the same way as c_c. It is used to find a spray cone half-angle, $\gamma/2$ as an angle covering 75 % of the cumulative mean liquid mass flux using Eq. (3). For better insight see Fig. 9 - 12 below.

Fluorescence of Light Heating Oil

Natural fluorescence of LHO is utilized for PIV-PLIF measurements. Knowledge of basic characteristics of the fluorescence is required for regular setup of the measurement system. Measurements of fluorescence were done using spectrometer FLS 920 Edinburgh Instruments. Fig. 2 shows emission spectra for excitation wavelength 266 nm and 355 nm. Fluorescence maximum is 416 nm for both the cases. The wavelength 416 nm was used for illustration of the excitation wavelength influence on emission efficiency. The maximum fluorescence yield is seen at excitation wavelength 355 nm. Although this wavelength is optimum, the wavelength 266 nm was chosen for PIV-PLIF measurements as it enables easier separation of fluorescence signal from excitation signal using optical filters.

Lifetime of the fluorescence was measured for an excitation pulse with wavelength 266 nm and width of 7 ns. Results for emission wavelength 416 nm (corresponding to maximum luminescence) are seen at Fig. 3. The fluorescence decay is modeled using two-exponential function $I = 0.209+0.007e^{-t/7.16e-9} + 0.004e^{-t/1.87e-8}$ with the time constants τ_1 = (7.16±0.17) ns, τ_2 = (18.7±0.2) ns. The values τ_1 and τ_2 are negligible in relation to the time scales of the PIV measurements. These results justify the usage of the natural fluorescence of LHO for both the PIV and PLIF. Dosing by a fluorescent dye would not probably bring any significant improvement in the measurement but it could lead to complications regarding to needed uniformity of dispersion in the LHO. Fluorescence signal was found to have linear relation with the excitation intensity in whole range of laser power used with no variation in the shape of emission spectra curve.

PLIF Corrections

Laser light passing through droplets is particularly reflected, transmitted and absorbed. Light scattered by droplet is then absorbed again on the path to camera in the spray. It is important to account for these effects. Our results are corrected for attenuation of laser light on its path into the spray according Beer-Lambert law [16]. Compensated intensity of the pixel i, I_i', is:

$$I_i' = I_i \exp\left(K \sum_{j=0}^{j=i-1} I_j'\right) \qquad (4)$$

where I_i is the observed pixel intensity and the constant K is found experimentally to obey spray axi-symmetry.

VELOCITY FIELD

Velocity distribution in the effervescent spray results from a discharge of compressed twin-fluid mixture. The gas, present in the mixture, exits the discharge orifice with high velocity (critical for pressure drop in the 10^5 Pa range and above) and rapidly expands shattering and accelerating

surrounding slower liquid into ligaments and droplets. Final droplets downstream decelerate by a still ambient air.

Fig. 4 shows a time-averaged velocity field of the atomizer E42. X-axis represents radial distance and Y-axis an axial distance from the exit orifice. Arrows show 2D velocity vectors of droplets and contours represents the velocity magnitude. Fig. 5, top, demonstrates a decrease of mean droplet axial velocity with the distance from the exit orifice. The stream in the spray axis keeps almost constant velocity while in higher radial distances the velocity decay is more significant due to mixing with surrounding air. Profiles of radial velocity (Fig. 5, bottom) show an abrupt change from positive to negative value near the spray axis and reach a maximum in the relative radial distance about 0.25.

Variation of relative radial velocity with relative radial distance is seen at Fig. 6. The relative radial velocity is taken as radial velocity divided by axial velocity and divided by relative radial distance. The value should be equal to -1 in the case when droplets follow straight path from the exit orifice. The actual relative radial velocity is generally lower. The relative radial velocity decreases with increase of axial distance near the spray axis but opposite tendency is seen near the spray borders. It means that the droplets tend to incline to the spray axis in larger axial distances and this tendency is more distinct in the spray axis. Droplets in higher radial distances are decelerated by surrounding air primarily in the axial direction. This conclusion is supported by a visual observation of the spray edge shape in [3] and also by velocity contour shape in Fig. 4, where a wrapping of the spray is seen.

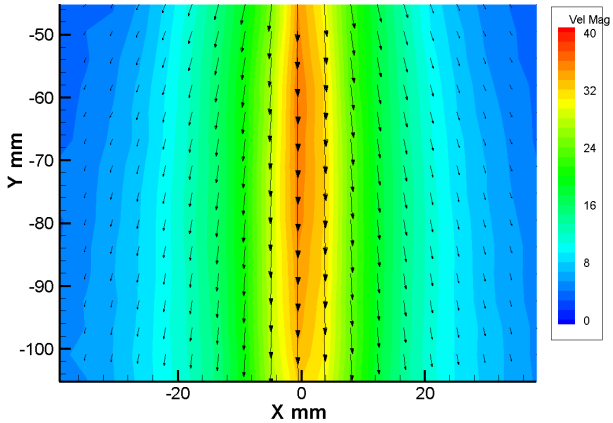

Fig. 4: Average velocity field, pressure 0.3 MPa, GLR 5 %.

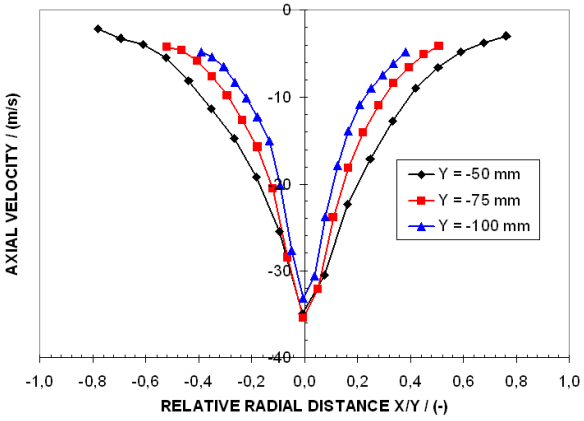

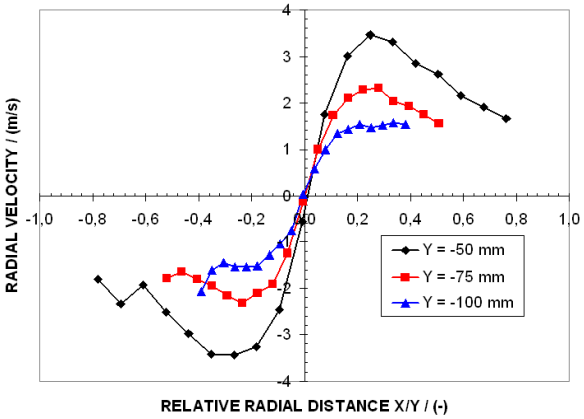

Fig. 5: Profiles of axial (top) and radial (bottom) velocity at different axial distances, inlet pressure 0.3 MPa, GLR 5 %.

Influence of the inlet pressure and GLR on the velocity magnitude is seen in Fig. 7. Increase of the pressure leads to an increase of velocity in entire profile. It is caused simply by higher discharge velocity of the mixture [17]. An increase in GLR leads not only to a change in velocity value but also to a change of the shape of velocity profile; lower GLR results in

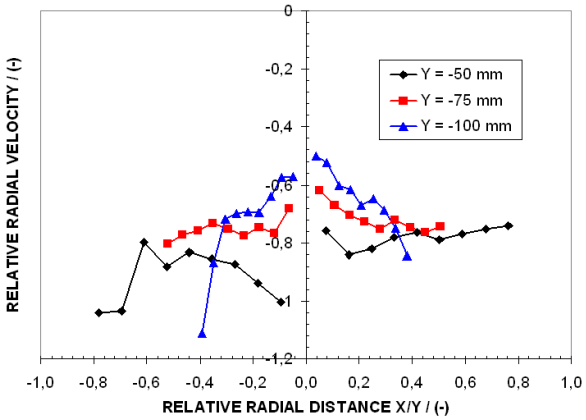

Fig. 6: Profiles of relative radial velocity at different axial distances, inlet pressure 0.3 MPa, GLR 5 %.

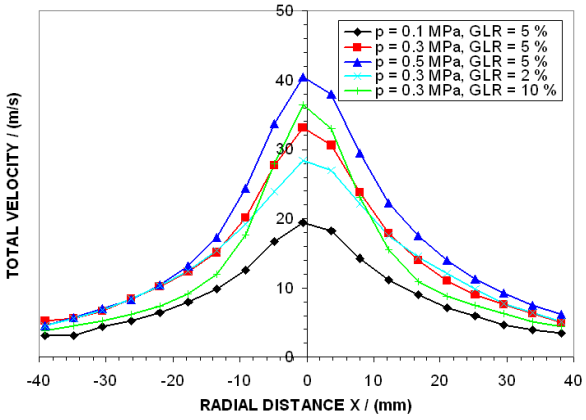

Fig. 7: Profiles of total velocity at axial distance 100 mm.

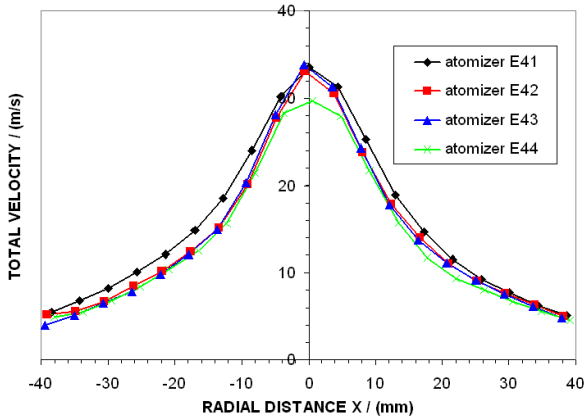

Fig. 8: Profiles of total velocity of different atomizers at inlet pressure 0.3 MPa, GLR 5 %, axial distance 100 mm.

more flat velocity profile. Increase of the velocity with increase in GLR is induced by greater aerodynamic drag force of the atomizing gas rather then by the increase of gas or liquid discharge velocity.

Fig. 8 gives an example of the influence of atomizer internal geometry on the velocity distribution. Length of the mixing chamber is changed using atomizers E41-E44. Shorter mixing chamber (E41) leads to slightly larger droplet velocity in whole radial profile. Influence of other geometrical parameters is similarly reasonable.

LIQUID CONCENTRATION WITHIN THE SPRAY

Spatial distribution of liquid concentration within the spray gives information about liquid-gas mixing ratio which is important in the combustion. Radial profiles of mean liquid concentration at axial distance 100 mm from exit orifice were acquired using planar LIF images of the concentration as described above. Fig. 9 documents radial profiles of the mean liquid concentration in the spray of atomizer E42. Spray is axially symmetrical with maximum of the concentration near the spray centerline; the concentration steeply declines with increasing radial distance. Inflection point is found in the distance 30 - 40 mm from the centerline depending on operation conditions. Note relatively rough profile at the pressure 0.1 MPa, where even average of 256 images was not enough to smooth out the influence of individual large droplets. The radial concentration profiles were used for calculation of the normalized cumulative concentration of liquid according to Eq. (2). Results on Fig. 10 show about 50 % of the liquid mass present in the cross section with the radius about 20 - 23 mm depending on operation conditions. More then 90 % of the liquid mass is covered inside the circle with 42 mm radius for all cases. A radial distance covering 75 % of the total liquid mass was used for determination of the spray cone width with respect to the concentration distribution. Resulting half-angle, $\alpha/2$, calculated according Eq. (3), for different atomizers and operation conditions is documented in Tab. 2. Influence of the injection pressure, p, is evaluated at 0.1, 0.3 and 0.5 MPa with GLR = 5 %. Influence of GLR at 2, 5 and 10 % is measured with the input pressure set to 0.3 MPa. The five investigated design parameters are described by a nondimensional relative values acquired by a comparison with some characteristic atomizer dimension.

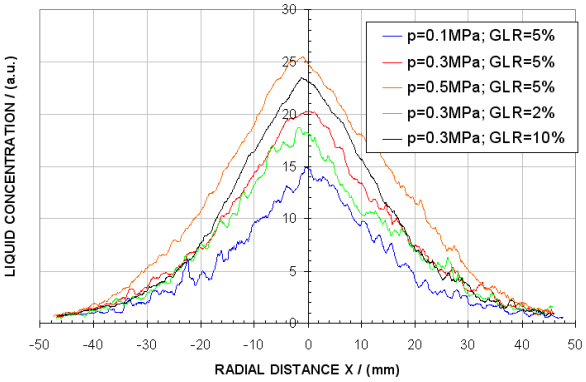

Fig. 9: Radial profiles of mean liquid concentration.

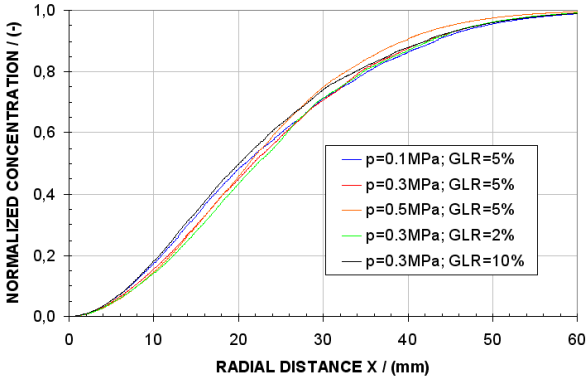

Fig. 10: Radial profiles of norm. cumulative concentration.

Results for different nozzles are very similar; the only exception is atomizer E56 with exit orifice in the shape of Laval nozzle. This atomizer gives significantly lower cone half-angles than other atomizers and is not considered in the comparison. The half-angles of all other atomizers show monotonous decrease with increasing GLR; the decrease is 1.4° for change of GLR between 2 and 10 % in the average. The same tendency was examined earlier in [2] where continuing reduction of the cone angle is noted at GLR 20 % and higher. The cone half-angles of particular atomizers range between 16.3° - 20.4° at GLR 2 % and 15.4° - 19.3° at GLR 10 %. The smallest drop in the cone half-angle in the measured range of GLR was 0.7° for atomizer E54, the greatest was 2.5° for E46.

Tests made at constant GLR, 5 % with operation pressure varied do not show so consistent tendency. Increase of the pressure mostly leads to a decrease of concentration angle. Some atomizers (E45, E48-E50) show the decrease only between pressure 0.1 MPa and 0.3 MPa and increase or stagnation between 0.3 MPa and 0.5 MPa. Atomizers E43,

Table 2. Half-angles of liquid concentration, $\alpha/2$ (deg).

Atom.	X^a (-)	p = 0.3 MPa			0.1 MPa	0.5 MPa
		2 %	10%	GLR = 5%		
	r_{lc}	Relative mixing distance $r_{lc} = l_c/d_c$				
E41	2.4	19.2	18.1	18.8	20.1	18.2
E42	3.8	18.0	17.1	17.7	18.1	17.0
E43	5.9	17.2	16.1	16.8	16.7	16.6
E44	7.4	16.3	15.6	16.3	16.8	16.2
	r_{dc}	Relative mixing chamber diameter $r_{dc} = d_c/d_o$				
E45	2.4	17.8	15.5	16.6	17.5	17.2
E46	3.2	18.1	15.6	16.5	15.8	17.0
E47	5.6	17.9	15.6	16.6	16.6	16.5
	r_a	Relative aeration area $r_a = n(d_a/d_o)^2$				
E48	0.017	17.6	16.0	16.9	17.4	17.1
E49	0.056	16.8	15.7	16.5	17.3	17.1
E50	0.077	16.8	15.4	16.0	16.9	17.2
	r_n	Relative area of single aeration hole $r_n = 1/n$				
E51	6.40	19.6	18.5	19.4	21.4	18.4
E52	3.84	19.1	17.6	18.6	20.6	18.2
E53	1.92	18.4	16.9	17.8	19.6	17.5
E54	1.28	17.8	17.2	17.7	19.2	17.1
	r_o	Relative length of the exit orifice $r_o = l_o/d_o$				
E55	0.16	19.9	19.0	19.6	20.1	17.8
E56	1.60	11.4	9.7	10.0	16.1	8.8
E57	1.20	17.8	15.4	17.1	18.7	16.4
E58	0.08	20.4	19.3	20.3	22.0	19.9

[a] X means nondimensional parameter varied during tests.

E46 and E47 perform yet more unlikely. Difference between individual atomizers is more distinct at low input pressure 0.1 MPa with the smallest half-angle 15.8° for E46 and the greatest 22° for E58 then at high pressure 0.5 MPa with the smallest half-angle 16.2° and the greatest 19.9°. Next paragraphs document influence of different geometric parameters on the concentration cone half-angle.

Exit nozzle shape: Atomizers E55, E57 and E58 have different length of exit orifice. Increase of the length/diameter ratio of the exit orifice, r_o, causes a constriction of the spray cone; Increase of r_o from 0.08 (E58) to 1.2 (E57) reduces the spray concentration angle by 2.6° - 3.9° depending on GLR and input pressure. Usage of a Laval nozzle (E56) instead of the plain nozzle improves a conversion of pressure energy to kinetic energy of the discharged mixture. It significantly influences the liquid distribution, the spray tend to be markedly narrower in this case.

Mixing chamber length: Atomizers E41-E44 have varying position of the aeration holes relative to the exit orifice. Distance between the last row of aeration holes and the exit orifice defines a length of the mixing chamber, l_c. Atomizer E41 with short relative mixing chamber length, r_{lc}, gives wider spray cone half-angle by 2.0° - 3.2° then atomizer E44 with larger r_{lc}. Long mixing channel probably leads to bubble merging and finally to worse mixing. Discharge of the mixture with larger volumes of separated phases results in the reduced exchange of energy between gas and liquid; expansion of gas volumes in this case does not contribute to the acceleration of liquid phase so effectively. Expansion of the gas behind the exit orifice in the well mixed case (short mixing channel) moves the liquid ligaments and droplets off the spray axis more easily. This assumption is supported by the velocity data (Fig. 8); atomizers with shorter mixing chamber show slightly higher droplet velocity in entire radial profile.

Aeration area: Atomizers E51-E54 have different number of aeration holes and hence varied aeration cross-section area relative to the exit orifice area, r_a. Atomizer E51 with large relative aeration cross-section area, r_a = 6.4, produces concentration half-angle wider by 1.3° - 2.2° compared to atomizer E54 with r_a = 1.3. Larger aeration area could probably improve mixing of gas with liquid and lead to better exchange of the compressed gas energy to the liquid desintegration work. However it is important to note that the variation of the aeration hole number of the atomizers E51-E54 was connected with a variation in the length of the mixing chamber. Results of the atomizers E41-E44 above show that the influence of the mixing chamber length is dominant.

Aeration chamber diameter (E45-E47): Cross section size of the mixing chamber controls the velocity of the mixture and resulting two-phase flow pattern. Results show influence of the mixing chamber diameter is relatively small compared to other factors and it is not consistent. Differences between atomizers are 0.1° - 1.7° depending on operation conditions.

Aeration hole diameter (E48-E50): Size of aeration holes controls the penetration of gas into liquid and final size of bubbles in the case of bubbly flow regime. Tab. 2 shows that atomizer E48 with aeration holes 0.6 mm produces by 0.1°-0.9° wider spray then atomizer E50 with holes 1.5 mm in diameter.

LIQUID MASS FLUX AND SPRAY CONE ANGLE

Spatial distribution of liquid flux in the spray gives important information about liquid transport within the spray. In the case of reacting spray the liquid distribution influences combustion process and resulting exhaust gas emissions. Radial profiles of mean liquid mass flux in the nozzle axial direction for atomizer E42 are described in Fig. 11. The radial profiles are measured in axial distance 100 mm from the nozzle exit. Shape of the flux profiles is similar to the shape of concentration profiles; they are axi-symmetric with a maximum in the spray centerline. The flux profiles are narrower then concentration profiles due to weighting by axial velocity. Cumulative distribution of the liquid flux, calculated according to Eq. (2), show that 50 % of the liquid flow is concentrated inside a circle with radius of 12 - 16 mm depending on operation conditions. 90 % of the flow is covered within radius of 28 - 31 mm (Fig. 12). The cumulative distribution of liquid flux was used for evaluation of the spray cone half-angle, $\gamma/2$, using Eq. (3) above.

Tab. 3 documents the spray cone half-angles of different atomizers operated at varied injection pressure and GLR similarly as in the previous table for concentration half-angles. All tested nozzles show very similar influence of GLR on the spray cone angle. The spray cone angle decreases as the GLR increases and the decrease is steeper at higher GLR. The average decrease of the spray cone half-angle is 1.9° for increase of GLR from 2 % to 10 %. This value is higher then the average decrease 1.4° in the case of half-angle of concentration. It reflects the variation of axial velocity profile with GLR (see Fig. 7 above). The cone half-angles of particular atomizers range between 10.5° - 14.4° at GLR 2 % and 8.8°- 11.9° at GLR 10 %.

Similarly as in the case of the liquid concentration half-angle, $\alpha/2$, also in the case of the spray cone half-angle, $\gamma/2$, the influence of the pressure is not uniform for all the atomizers. The tendency is a decrease of the spray cone angle with the pressure increase for about one half of the atomizers, but atomizers E42, E44, E45 and E48-E50 show the decrease of cone half-angle only between 0.1 and 0.3 MPa and increase

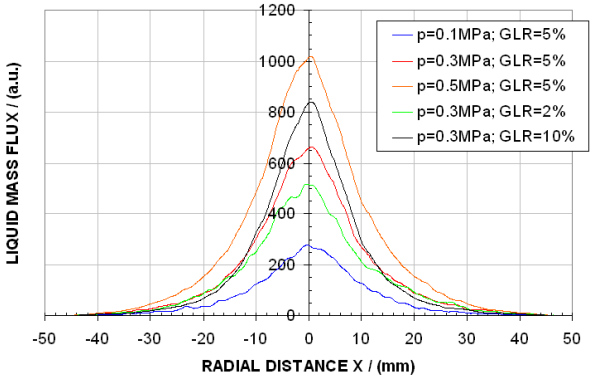

Fig. 11: Radial profiles of mean liquid mass flux.

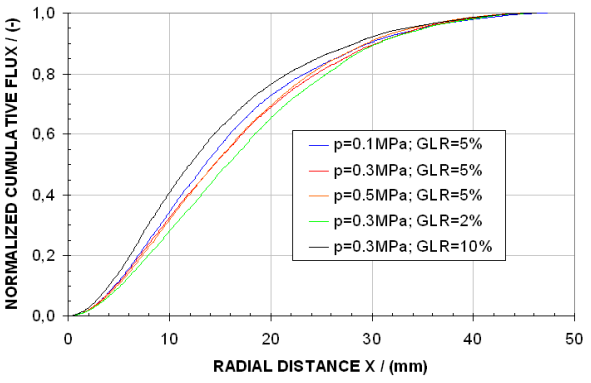

Fig. 12: Radial profiles of normalized cumulative mean liquid mass flux.

between 0.3 and 0.5 MPa. The cone half-angle for atomizers E46, E47 and E57 increases with the pressure increase in whole pressure range. There is no simple explanation for this divergent behaviour. Influence of different geometric parameters of effervescent atomizer on the spray cone half-angle is described in the following section. The description is made briefly as most things were already explained above.

Exit nozzle shape: Larger length/diameter ratio of the exit orifice, r_o, leads to more narrow spray regardless to operation conditions. Increase of r_o from 0.08 to 1.2 reduces the spray cone half-angle by 2.7° - 4.8° according to operation conditions. The longer orifice the better streamline of the mixture, turbulence is then reduced and axial velocity is preferred resulting in lower spray cone angle. Laval nozzle (E56) produces extremely narrow spray cone. Such orifice shape can be useful in applications where concentrated spray or spray with higher axial velocity is desired. Better energy transfer in the Laval nozzle could also lead to finer drop size compared to the plain orifice.

Aeration hole position: Atomizer E41 with short mixing chamber (r_{lc} = 2.4) gives wider spray cone half-angle by 0.8° - 3.0° then atomizer E44 with long mixing chamber (r_{lc} = 7.5) depending on the pressure and GLR. The difference in the spray cone half-angle is larger for low pressure and for low GLR. This tendency follows from the spray concentration distribution where similar tendency is observed (see above).

Aeration area: Change of relative aeration area, r_a, from 1.3 to 6.4 causes increase of the spray cone half-angle by 0.8° - 1.6° in overall range of GLR and input pressure.

Table 3. Spray cone half-angles, $\gamma/2$ (deg).

Atom.	X^a (-)	p = 0.3 MPa			0.1 MPa	0.5 MPa
		2 %	10%	GLR = 5%		
	r_{lc}	Relative mixing distance $r_{lc} = l_c/d_c$				
E41	2.4	14.1	10.9	13.6	14.6	13.1
E42	3.8	13.3	11.1	12.7	12.1	12.5
E43	5.9	12.0	10.0	11.9	12.2	11.6
E44	7.4	11.4	10.1	11.3	11.6	11.7
	r_{dc}	Relative mixing chamber diameter $r_{dc} = d_c/d_o$				
E45	2.4	12.1	10.2	11.4	12.3	11.7
E46	3.2	11.9	10.7	11.8	10.9	12.6
E47	5.6	12.2	10.2	11.5	11.0	12.0
	r_a	Relative aeration area $r_a = n(d_a/d_o)^2$				
E48	0.017	11.8	10.3	11.6	12.2	12.0
E49	0.056	11.9	10.1	11.3	11.7	11.9
E50	0.077	11.8	9.7	11.0	11.4	11.6
	r_n	Relative area of single aeration hole $r_n = 1/n$				
E51	6.40	13.5	11.6	13.1	13.6	12.6
E52	3.84	12.9	10.8	12.3	13.0	12.0
E53	1.92	12.6	10.5	11.9	12.4	11.8
E54	1.28	12.2	11.1	11.8	12.0	11.8
	r_o	Relative length of the exit orifice $r_o = l_o/d_o$				
E55	0.16	13.9	11.6	13.2	13.7	13.0
E56	1.60	5.2	4.9	5.1	5.2	5.2
E57	1.20	10.5	8.8	10.1	9.6	10.2
E58	0.08	14.4	11.9	13.8	14.4	13.0

[a] X means nondimensional parameter varied during tests.

Aeration chamber diameter: Influence of the mixing chamber diameter on the mass flux is similar to the influence on concentration - relatively small compared to other factors and ambiguous. Maximum difference between particular atomizers is 0.3° - 1.4° depending on operation conditions.

Aeration hole diameter: Influence of the size of aeration holes on the spray cone half-angle is relatively small. Atomizer E48 with 0.6 mm aeration holes gives by 0.1° to 0.8° wider spray cone half-angle then atomizer E50 with 1.5 mm aeration holes.

Direct relation between half-angles covering 75 % of the liquid flow and half-angles for 90 % of the liquid flow in Fig. 13 declares that the distribution of liquid mass is influenced in different radial distances similarly.

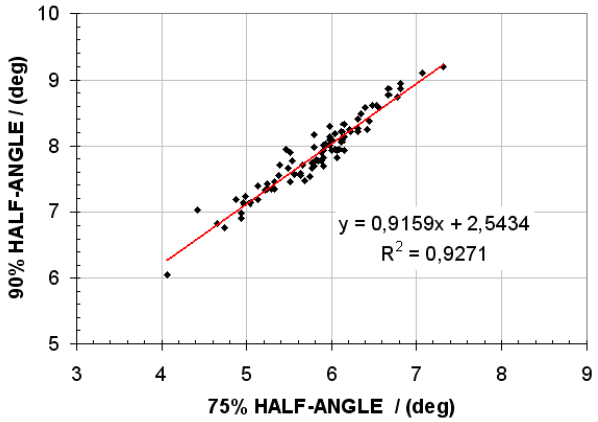

Fig. 13: Correlation between half-angles for 75 % of the liquid flow and half-angles for 90 % of the liquid flow.

CONCLUSIONS

The study of effervescent spray using PIV-PLIF technique gives information on spatial distribution of droplet velocity, liquid concentration and liquid mass flux within the spray. Main conclusions are:

1. Radial profiles of axial droplet velocity are bell-shaped with a maximum in the spray centerline. The spray near the centerline keeps almost constant velocity, while droplets in larger radial distances decelerate markedly due to mixing with surrounding air. Atomizer operation conditions significantly influence the velocity magnitude. Increase of the injection pressure causes an increase of velocity in entire radial profile. Increase in GLR leads not only to change of velocity value but also to a change of the velocity profile shape; lower GLR results in more flat profile. Influence of atomizer internal geometry on the droplet velocity distribution is reasonable.
2. Radial profiles of liquid concentration in the spray are axi-symmetrical with maximum near the spray centerline; the concentration steeply declines with increasing radial distance. Cone half-angle, $\alpha/2$, in the spray, which includes 75% of the liquid mass, shows monotonous decrease with increasing GLR for all atomizers. The cone half-angle of particular atomizers range between 16.3° - 20.4° at GLR 2 % and 15.4°- 19.3° at GLR 10 %. Increase of the injection pressure in the range 0.1 - 0.5 MPa mostly leads to a decrease of $\alpha/2$, but several atomizers behaves differently. The concentration half-angle increases with decrease in length/diameter ratio of the exit orifice, with decrease in the mixing chamber length, with increase in aeration area and with decrease in the aeration hole diameter. Influence of the aeration

chamber diameter is relatively small compared to other factors and it is not consistent.

3. Spatial distribution of liquid flux in the spray is similar to the distribution of concentration, but the radial flux profiles are narrower then concentration profiles. Spray cone half-angle, $\gamma/2$, of all atomizer decreases as the GLR increases and the decrease is steeper at higher GLR. The average decrease of the spray cone half-angle is 1.9° for increase of GLR from 2 % to 10 %. The cone half-angles of particular atomizers range between 10.5° - 14.4° at GLR 2 % and 8.8° - 11.9° at GLR 10 %. Influence of injection pressure is not uniform for different atomizers. Influence of the atomizer internal geometry on the spray cone half-angle, $\gamma/2$, is generally the same as for the concentration half-angle, $\alpha/2$, described above.

KEYWORDS

Effervescent Atomization, Liquid Concentration, Liquid Flux, Spray Structure, Droplet Velocity, PIV-PLIF, spray cone half-angle

ACKNOWLEDGMENT

Authors greatly acknowledge financial support from project GA 101/06/0750 funded by the Czech grant agency.

NOMENCLATURE

Symbol	Quantity	SI Unit
c	Liquid concentration	kg/m^3
c_c	Normalized liquid conc. distribution	-
d_a	Aeration hole diameter	mm
d_c	Mixing chamber diameter	mm
d_o	Exit orifice diameter	mm
GLR	Gas to liquid ratio by mass	-
I	Light intensity	W/m^2
i, j	Indices	-
l_c	Length of the mixing chamber	mm
l_o	Length of the exit orifice	mm
K	Attenuation constant	-
$\dot{m}$	Liquid mass flux	kg/m^2 s
$\dot{m}_c$	Norm. cumulative liquid mass flux	-
n	Number of aeration holes	-
p	Injection pressure	MPa
r	Radial distance from spray centerline	mm
r_a	Relative aeration area	-
r_{dc}	Relative mixing chamber diameter	-
r_{lc}	Relative mixing distance	-
r_n	Relative area of single aeration hole	-
r_o	Relative length of the exit orifice	-
x, y	Radial and axial coordinates	mm
w	Axial velocity	m/s
α	Concentration angle	deg
β	Apical angle in front of the exit orifice	deg
γ	Spray cone angle	deg
Δl	Length of aeration area	mm
τ	Time constant	s

REFERENCES

[1] J.D. Whitlow and A.H. Lefebvre, Effervescent Atomizer Operation and Spray Characteristics, *Atomization and Sprays*, Vol. 3, pp. 137-155, 1993.

[2] J. Jedelsky and M. Jicha, Unsteadiness in Effervescent Sprays - Measurement and Evaluation using Combined PIV-PLIF Technique, *Proc. 13th Int. Symp. on Appl. of Laser Techniques to Fluid Mech.*, pp. 1-10, 2006.

[3] S.K. Chen and A.H. Lefebvre, Spray Cone Angles of Effervescent Atomizers, *Atomization and Sprays*, Vol. 4, pp. 291-301, 1994.

[4] R.A. Wade, J.M. Weerts, P.E. Sojka, J.P. Gore and W.A. Eckerle, Effervescent Atomization at Injection Pressures in MPa Range, *Atomization and Sprays*, Vol. 9, pp. 651-667, 1999.

[5] S.D. Sovani, J.D. Crofts, P.E. Sojka, J.P. Gore and W.A. Eckerle, Structure and Steady-State Spray Performance of an Effervescent Diesel Injector, *Fuel*, Vol. 84, pp. 1503-1514, 2005.

[6] S.D. Sovani, E. Chou, P.E. Sojka, J.P. Gore, W.A. Eckerle and J.D. Crofts, High Pressure Effervescent Atomization: effect of ambient pressure on spray cone angle, *Fuel*, Vol. 80, pp. 427-435, 2000.

[7] S.D. Sovani, P.E. Sojka and A.H. Lefebvre, Effervescent Atomization, *Progress in Energy and Comb. Science*, Vol. 27, Issue 4, pp. 483-521, 2001.

[8] J. Jedelsky, M. Jicha, J. Otahal and M. Landsmann, Design of Effervescent Atomizer for Industrial Oil Burner, *Proc. Symp. 9th FLUCOME*, 2007.

[9] J.J. Sutherland, P.E. Sojka and M.W. Plesniak, Ligament Controlled Effervescent Atomization, *Atomization and Sprays*, Vol. 7, pp. 383-406, 1997.

[10] P.J. Santangelo and P.E. Sojka, A Holographic Investigation of the Near Nozzle Structure of an Effervescent Atomizer Produced Spray, *Atomization and Sprays*, Vol. 5, pp. 137-155, 1995.

[11] J. Wang, X-ray Visions of Multiphase Flow, *Proc. 13th Int. Symp. on Appl. Laser Tech. to Fluid Mech.*, 2006.

[12] J.V. Pastor, J.J. López, J.E. Juliá, Planar Laser-Induced Fluorescence Fuel Concentration Measurements in Isothermal Diesel Sprays, *Optics Express*, Vol. 10, Issue 7, pp. 309-323, 2002.

[13] M.V. Panchagnula and P.E. Sojka, Spatial Droplet Velocity and Size Profiles in Effervescent Atomizer-Produced Sprays, *Fuel*, Vol. 78, pp. 729-741, 1999.

[14] J. Jedelsky, M. Jicha and J. Slama, Characteristics and Behaviour of Multi-Hole Effervescent Atomizers, *Proc. Symp. 19th ILASS Europe*, pp. 521-526, 2004.

[15] J. Jedelsky and M. Jicha, Unsteadiness in Effervescent Sprays - a New Evaluation Method and the Influence of Operational Conditions, *Atomization and Sprays*, Vol. 18, pp. 49-83, 2008.

[16] R. Abu-Gharbieh, J. Persson, M. Försth, A. Rosén, A. Karlström and T. Gustavsson, Compensation Method for Attenuated Planar Laser Images of Optically Dense Sprays, *J. of Applied Optics*, Vol. 39, No. 8, pp. 1260-1267, 2000.

[17] J.C. Leung and M. Epstein, A Generalized Correlation for Two-Phase Non-Flashing Homogeneous Choked Flow, *ASME J. of Heat Transfer*, pp. 528-530, 1990.